J Mater Sci (2018) 53:10122–10134

Composites

Implementation of functionalized multiwall carbon nanotubes on magnetorheological elastomer

Siti Aishah Abdul Aziz[1], Ubaidillah[2], Saiful Amri Mazlan[1,*], Nik I. Nik Ismail[3], and Seung-Bok Choi[4,*]

[1] *Vehicle System Engineering, Malaysia – Japan International Institute of Technology (MJIIT), Universiti Teknologi Malaysia (UTM), 54100 Kuala Lumpur, Malaysia*
[2] *Department of Mechanical Engineering, Faculty of Engineering, Universitas Sebelas Maret, Surakarta, Indonesia*
[3] *Advanced Processing and Product Technology Centre R&D Centre of Excellence (COE), Malaysian Rubber Board, Experimental Station, 47000 Sg Buloh, Selangor, Malaysia*
[4] *Department of Mechanical Engineering, Inha University, 253, Yonghyun-dong, Namgu, Incheon 402-751, Korea*

Received: 25 December 2017
Accepted: 9 April 2018
Published online: 16 April 2018

ABSTRACT

This work studies the effects of loading various functionalized multiwall carbon nanotubes (carboxyl, –COOH-MWCNTs) on the morphological and the field-dependent rheological properties of magnetorheological elastomers (MREs). A new type of MRE, which is reinforced by various loading from 0 to 1.5 wt% of COOH-MWCNT, is fabricated and experimentally investigated. The morphology of COOH-MWCNT and MRE with COOH-MWCNTs is characterized using field emission scanning electron microscopy and transmission electron microscopy. The results indicate that the COOH-MWCNTs are well embedded and dispersed randomly in the MRE structures. The rheological properties under different magnetic fields are evaluated using parallel plate rheometers. The influence of COOH-MWCNT content on the viscoelastic performance of the MRE is systematically investigated. It is found that when a higher content of COOH-MWCNT (up to 1.0 wt%) is added in the MRE, the MRE exhibits a higher MR effect of up to 17.5%. It is also shown that COOH-MWCNT acts as a reinforcing agent that leads to an enhancement in MR performance.

Abbreviation

MR	Magnetorheological
MRE	Magnetorheological elastomer
MRF	Magnetorheological fluid
MRG	Magnetorheological grease
NR	Natural rubber
SMR	Standard Malaysia rubber
CIP	Carbonyl iron particle
COOH-MWCNT	Carboxyl multiwall carbon nanotubes
EPO	Epoxidized palm oil
G'	Storage modulus
G'_0	Storage modulus (without magnetic field)
FESEM	Field emission scanning electron microscopy

Address correspondence to E-mail: amri.kl@utm.my; seungbok@inha.ac.kr

https://doi.org/10.1007/s10853-018-2315-3

TEM	Transmission electron microscopy
MRD	Magnetorheological device
ΔG	Magneto-induced modulus

Introduction

For the last two decades, magnetorheological (MR) materials such as MR fluids (MRFs), MR elastomers (MREs), MR grease (MRG) and MR foam have been extensively studied as smart materials for vibration/impact control or position control in both industrial and academic areas due to their inherent characteristics, such as property controllability with a fast response time [1–10]. Among those smart materials, MRE has attracted the most interest since it exhibits a desirable performance due to the stability of the magnetizable particles in the matrix. It also involves simpler material handling, without leaking or sedimentation [11, 12]. MREs always operate in a pre-yield regime, as the field-dependent modulus is usually used to characterize the strength of the responsive field. MREs mainly consist of rubber as a matrix, and ferromagnetic particles. Several researchers have found that the critical factors that affect MRE properties are matrix material, magnetizable particles and additives [13–17]. In the stage of synthesizing a MRE, the selection of matrix plays an important role as it contributes to its mechanical and rheological behaviour. This, in turn, would affect its design and performance. Generally, rubber is used as a matrix in MRE due to its high and reversible deformability [18]. In addition, rubber consists of polymer chains, which are frequently used to interlock the magnetic particles during curing [19]. Several types of rubber, including natural rubber (NR) [20, 21], epoxidized natural rubber (ENR) [2, 22, 23] and silicone rubber (SR) [24–28], are widely used as matrix for MREs [29–31]. Rubber is an originally non-magnetic material whose modulus properties are constant throughout any applied magnetic field. Since the essential modulus and strength of neat rubber is low, an additional reinforcing phase is necessary for the practical use of MRE materials. Carbon black (CB) is frequently used as filler when fabricating the MRE. Chen et al. [33] fabricated different ratios of 0–7% of CB on anisotropic MRE based on NR samples. The study has shown that the MRE samples with 7% of CB have a higher relative and absolute MR effect (104%) as compared to other samples. Furthermore, the addition of CB as an additive lead to a well-bound microstructure resulting in improvement in mechanical properties and lower damping ratios.

Apart of CB, there are a few other fillers have been explored recently by researchers to obtain an optimum performance of the MR effect for various applications, especially in vibration isolators [20, 32, 33]. For instance, the addition of montmorillonite and SiC nanoparticles into rubber shows that some improvements in the mechanical properties and affect also contribute to the MRE performance [20, 33, 37–39]. Wang et al. developed a group of MREs with different contents of 60-nm SiC nanoparticles: 0, 1, 2, 3, 4 and 5 wt% as an additive. The MR effect, the maximum storage modulus and the magneto-induced storage modulus increased when the SiC content reached 4 wt% and decreased sharply after the SiC nanoparticle content exceeded 4 wt% [46]. Besides filler, plasticizer is also an important additive in improving MRE performance. Khairi et al. [22] fabricate MRE with 60 wt% CIP and with various loading of 0–10% sucrose acetate isobutyrate ester (SAIB) as an additive in order to soften the matrix and improve the MRE performance. The results revealed that with the addition of 7.5% SAIB, the MR effect increased up to 22.9%. The physicochemical of MREs was enhanced with the addition of SAIB ester which showed that the softer matrix helped to homogenously disperse the CIP during the mixing process.

Currently, nanoparticles have attracted the attention of researchers due to their high surface area and their strongly interconnectivity in three-dimensional networks at relatively low filler loadings [34–38]. To this end, few investigations involving small magnetic filler loading of nanoparticles have been carried out in MREs. Landa et al. fabricated 2% of 360 nm of nickel nanoparticles and nanochains in MRE samples. Their study revealed that the anisotropy effects in both magnetic and elastic properties in the magnetorheological PDMS-Ni composites are larger when using nanochains as fillers [39]. Meanwhile, Li et al. [37] fabricated 20% CIP with 1 wt% of multiwall carbon nanotubes (MWCNT) and the authors found that the initial modulus increased as MWCNT loading increased compared to conventional MREs. Further, the author continued to investigate the dynamic

mechanical response of MR nanocomposites using 1 and 3.5 wt% of MWCNT in RTV silicone rubbers. At all dynamic compression and shear tests, MR nanocomposites showed higher zero-field stiffness and damping along with greater magnetic field-induced increasing dynamic mechanical properties, especially with 1 wt% of MWCNT. However, with an addition of 3.5 wt% of MWCNT, the MRE did not constantly exhibit higher dynamic stiffness and damping properties as compared to 1.0 wt% MWCNT which most likely resulted from the defects of specimens due to fabrication issues [36]. Aziz et al. investigated the viscoelastic properties of different types of MWCNT and their effects on MR performance. The results have revealed that by adding 0.1 wt% of COOH-MWCNT, the magnetic properties are improved with parallel enhancement of MR effects, particularly at low strain amplitudes [40]. This is because functionalized carboxyl MWCNTs exhibit better interfacial bonding properties, and better dispersion compared to MWCNTs. It is known that the extent of the improvement generally depends on several parameters related to the additives including the aspect ratio, the state of dispersion and the surface chemical characteristics. These parameters determine the interaction between the filler/additive and the polymer chains, and thus the interface with the polymer-filler system [34, 35].

As reviewed from the above literature, a comprehensive assessment about the functionalized carboxyl MWCNT (COOH-MWCNT) needs to be further investigated. A study on various loadings of COOH-MWCNT as additives towards MREs and its optimum performance of COOH-MWCNT in terms of physicochemical and viscoelastic properties of MRE have not been reported yet in this research area. Consequently, the main technical contribution of this work is to investigate various loading of COOH-MWCNT for the fabrication of isotropic MREs and demonstrate the wide controllability of the field-dependent rheological properties. In order to achieve this goal, firstly, several samples of the NR-based MRE were fabricated using 0–1.5 wt% of COOH-MWCNT. Morphology of the COOH-MWCNT and the fabricated proposed MRE samples containing COOH-MWCNT have been analysed. Subsequently, the influences of the magnetic field, excitation frequency and strain amplitude of the field-dependent rheological properties of various loadings of COOH-MWCNT in MREs are thoroughly investigated through the dynamic oscillation shear test. It is shown that a controllable storage modulus and loss factor can be easily obtained by tuning the magnetic intensity and adjusting contents of COOH-MWCNT.

Samples preparation and test methods

Preparation of MREs

The natural rubber (NR) (SMR-20) produced by the Malaysian Rubber Board was used as a matrix for the MRE samples. Carbonyl iron particles (CIP) were utilized as magnetic particles with an average diameter of 6 μm and were purchased from BASF Germany. The functionalized multiwall carbon nanotubes (COOH-MWCNT) were supplied by Shenzhen Nanotech Port Co Ltd in China. The purity of COOH-MWCNT is $> 95\%$ and its outside diameter is 20 nm, respectively. The length of this COOH-MWCNT is 10–30 μm. Epoxidized palm oil (EPO) was applied as a medium to disperse CIP and MWCNTs. Sulphur was used as a vulcanization agent with other additives for MRE fabrication.

The COOH-MWCNT with different weight ratios of 0.1, 0.5, 1.0 and 1.5 wt% were sonicated in the epoxidized palm oil (EPO) (Rovpro 5301, Rovski Industries Sdn. Bhd) for 20 min with 4 s on and 2 s off pulse using the horn-type ultrasonicator (FB 705, Fisher Scientific (M) Sdn Bhd, Malaysia) to break the van der Waals interaction. Secondly, using the double-roll mill, 100 grams of NR was rolled between two 6-inch open rollers at a fixed temperature of 25° separated by 2.0 mm and moved through the roll mill for 10 min. Finally, rubber additives were then added into the mixer, followed by CIPs and COOH-MWCNTs. The EPO was poured in the mix for 5 min. In order to avoid a premature cross-linking reaction, the sulphur and accelerator were put towards the end of the mixing process. Subsequently, the mixing was passed through the double-roll mill seven times for homogenization. The formulation of the MRE samples is given in Table 1.

Morphological and rheological characterization

The morphology of the COOH-MWCNT was examined through a transmission electron microscopy (TEM); Joel, JEM-2100 Plus, Japan with a

Table 1 Formulation of the MREs samples

Compounding ingredients	Weights (g)				
	MRE-1	MRE-2	MRE-3	MRE-4	MRE-5
SMR 20	100	100	100	100	100
ZnO[a]	5	5	5	5	5
Stearic acid	2	2	2	2	2
CIP (wt%)	30	30	30	30	30
COOH-MWCNT (wt%)		0.1	0.5	1.0	1.5
Epoxidized palm oil[b]	10	10	10	10	10
Santoflex 13[c]	1.5	1.5	1.5	1.5	1.5
Sulphur	2.5	2.5	2.5	2.5	2.5
CBS[d]	1	1	1	1	1

[a]Zinc oxide (activator)

[b]Processing oil

[c]Antiozonant and synthetic polymer stabilizer

[d]N Cyclohexylbenzothiazole-2-sulphenamide (accelerator) (Rubber and rubber additive supplied by Malaysian Rubber Board.)

magnification of 5000X at an accelerating voltage of 5 kV. The preparation sample of COOH-MWCNT was generally almost the same as reported by another researcher [41]. Some ethanol was dropped on the COOH-MWCNT films, and these films were transferred to the carbon-coated grip with a pair of tweezers. The MRE samples were prepared using Leica FC6 cryo-ultramicrotome. The sample was cut into slices of 60 nm thickness using a diamond knife. In addition, the field emission scanning electron microscopy (FESEM); Supra 40VP-31-31, Germany. The samples were coated with gold for the FESEM analysis and analysed by using 2000× magnification at the accelerating voltage of 2 kV.

Rheological behaviours of the fabricated MRE samples were examined by using an MR device (MRD 170) in the oscillation state (Physica MCR 302, Anton Paar, Germany). Circular samples with a diameter of 20 mm and thickness of 1 mm were prepared and subjected to shear tests using a rotary disc with frequency sweep tests from 0.1 to 100 Hz with a constant strain of 0.06% and strain sweep tests from 0.01 to 25% with a constant frequency of 1 Hz. The magnetic fields were varied in the intervals of 0, 1, 2, 3, 4 and 5A which correlate to 0, 186, 336, 508, 643 and 747 mT. The experiments were conducted at ambient temperature. The rheological experiments for all MRE samples were repeated three times to get consistent experimental results. The average from the data analysis was taken as a result of this study.

MR effect results and discussions

Morphological evaluation

Figure 1 shows the TEM images of COOH-MWCNTs. The COOH-MWCNTs show random curly or entangled structures and possess high aspect ratios with an outer diameter of about 20 nm. From the figure, the COOH-MWCNTs have a uniform diameter distribution and contain no obvious deformity in the structure. In addition, it can be noticed from the images that all the nanotubes are hollow cores with several layers of graphitic carbon and they are tubular in shape. The individual nanotubes can be highly entangled with one another and form interconnecting structures as shown in Fig. 1(b).

The TEM images of the cross-sectional cryofracture surface of the MRE samples with 0.1 wt% of COOH-MWCNT at 10,000× magnification are shown in Fig. 2. From the picture, the microstructure and dispersion of COOH-MWCNTs were observed. At higher magnifications, the individual nanotubes were clearly observed at low nanotube loadings. They are homogenously dispersed and distributed in MRE samples. Meanwhile, the prominent black regions visualized indicate an interlocking structure of bundles of COOH-MWCNTs which are similar to the ones previously reported by Petriccione et al. [42]. It is suggested that the COOH-MWCNTs were embedded, debundled and distributed throughout the matrix as a result of functionalized MWCNTs.

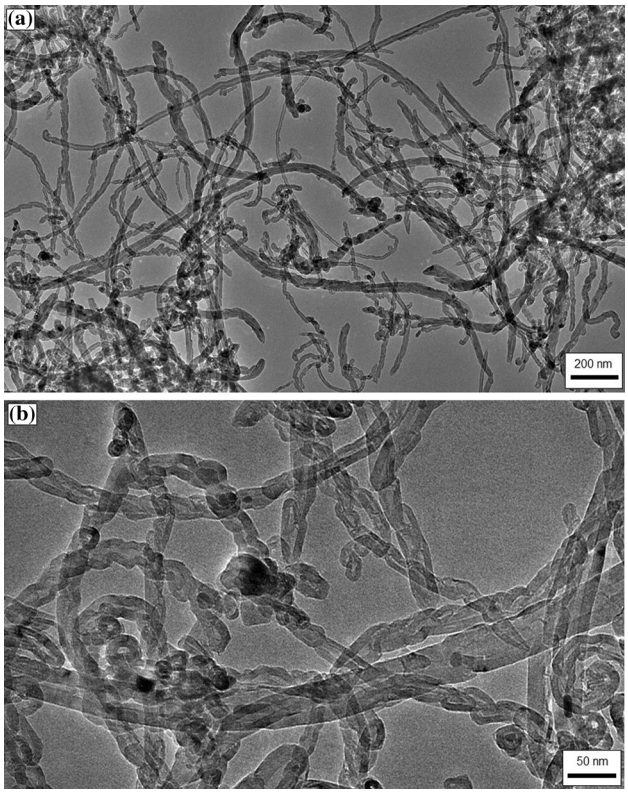

Figure 1 TEM images of COOH-MWCNT **a** at low resolution **b** at high resolution.

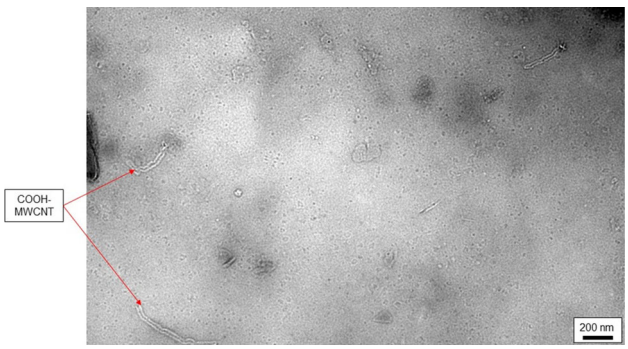

Figure 2 TEM images at 10,000× of COOH-MWCNT in MRE sample.

The results are in accordance with Qui et al. [43] in which the functionalized MWCNTs showed better dispersion and compatibility in rubber as compared to MWCNTs. The dispersion state of COOH-MWCNTs was one of the keys for the enhancement of rheological properties. Similar results have been reported by Kong et al. for TPNR/functionalized MWCNTs composite. The existing functional groups attached to the surface of MWCNTs react with the matrix during the curing process and contribute to improvements in the interfacial interaction. This leads to the composites having a higher strength and assists in increasing the dispersion and homogenization of the COOH-MWCNT in MREs [44].

Rheological properties of frequency swept of MRE

Figure 3 presents the frequency dependencies of the storage modulus for all MRE samples. It is apparent that the MRE without COOH-MWCNT exhibits a lower storage modulus at all frequency sweeps and magnetic field strengths as compared to MREs with different loadings of COOH-MWCNTs. Upon addition of 0.1–1.5 wt% of COOH-MWCNTs in MRE samples, all samples exhibit the increment of the initial storage modulus in the off state (from 3.4 to 5.49 MPa) and on state (0.5 T) from 4.3 to 5.5 MPa, respectively. Meanwhile, for the maximum storage modulus, the higher the COOH-MWCNTs content, the higher the increment of the storage modulus in off-state and on-state conditions which are shown in Fig. 3a, b, respectively. The increment of storage modulus towards the frequencies (0.1–100 Hz) and magnetic fields (0 and 0.5 T) resulted in the enhancement of bonding between COOH-MWCNTs, CIP and matrix which lead to the enhancement of storage modulus. The highest increment of storage modulus in the sweep frequency can be seen from the MRE with 0.5wt % of COOH-MWCNT, for which in the off-state condition, the initial storage modulus was 4.6 MPa and in the on-state condition, it increased to 5.0 MPa. However, when the increments of COOH-MWCNTs content go above 1.0 wt%, the initial storage modulus is approximately unchanged at its off-state and 0.5-T condition.

In contrast to the storage modulus that increased with the increasing of a magnetic field, the loss factor shows decreasing trend as the magnetic field increased. In the off-state condition, the MRE without COOH-MWCNTs showed unique findings as the loss factor is lower compared to MREs with 0.1 and 0.5 wt% COOH-MWCNTs. The increase in loss factor should be observed with an increase in the content COOH-MWCNTs, but this result is not observed in our work. The slight decrease in loss factors for MREs without COOH-MWCNTs might be related to the localized dispersion of CIPs in MREs, as reported by Silva et al. [45]. The presence of CIPs acts as an obstacle for the movement of molecular chains of

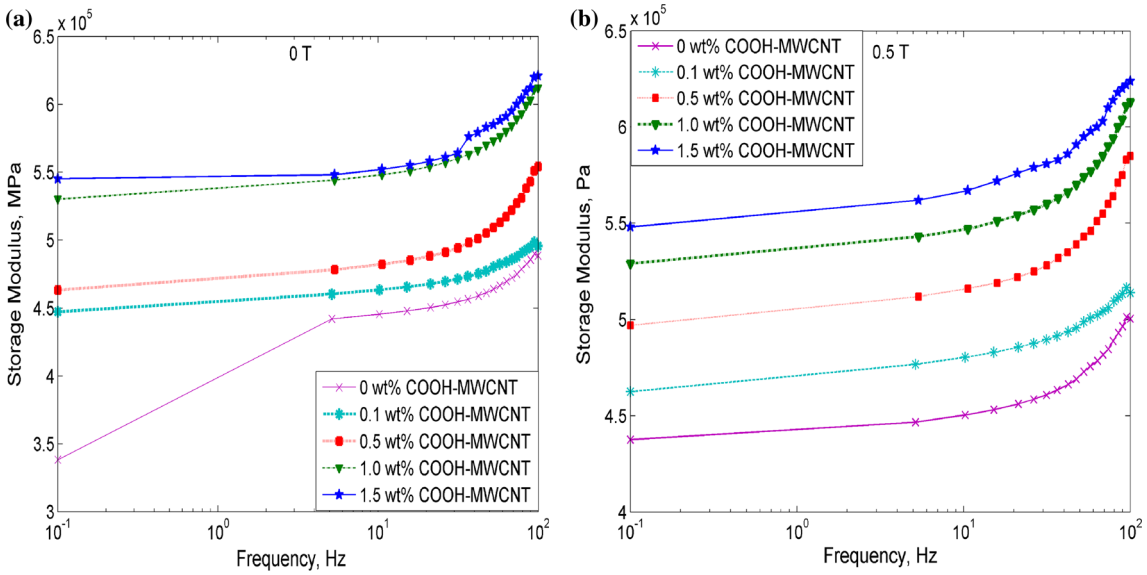

Figure 3 Storage modulus vs frequency at **a** 0 T and **b** 0.5 T for different ratios of COOH-MWCNT.

polymers in higher frequencies which leads to the decrement of loss factors as shown in Fig. 4. For instance, in Fig. 4b, the MRE with 0.1 wt% COOH-MWCNT exhibits a higher loss factor with an increment in frequency compared to the other samples. This is due to the agglomerations that appear, as reported in our previous report, which leads to a higher loss factor compared to MRE samples without COOH-MWCNT [46]. Nevertheless, at the on-state condition of 0.5 T, the loss factor of MRE samples with a 0.5–1.5 wt% content of COOH-MWCNT showed decrement trending at all frequencies compared to the off-state conditions. It is obvious to see that at higher frequencies above 10 Hz to 60 Hz, all the MRE samples exhibit higher loss factors compared to their off-state conditions. This phenomenon might be related to the role of COOH-MWCNTs as additives in the MRE samples. In this state, the COOH-MWCNT plays an important role due to the higher specific area and it is reasonable to assume that a higher content of COOH-MWCNT will lead to better rubber–filler interactions. Therefore, more energy dissipation of internal friction between the CIP and COOH-MWCNT phases occurred in

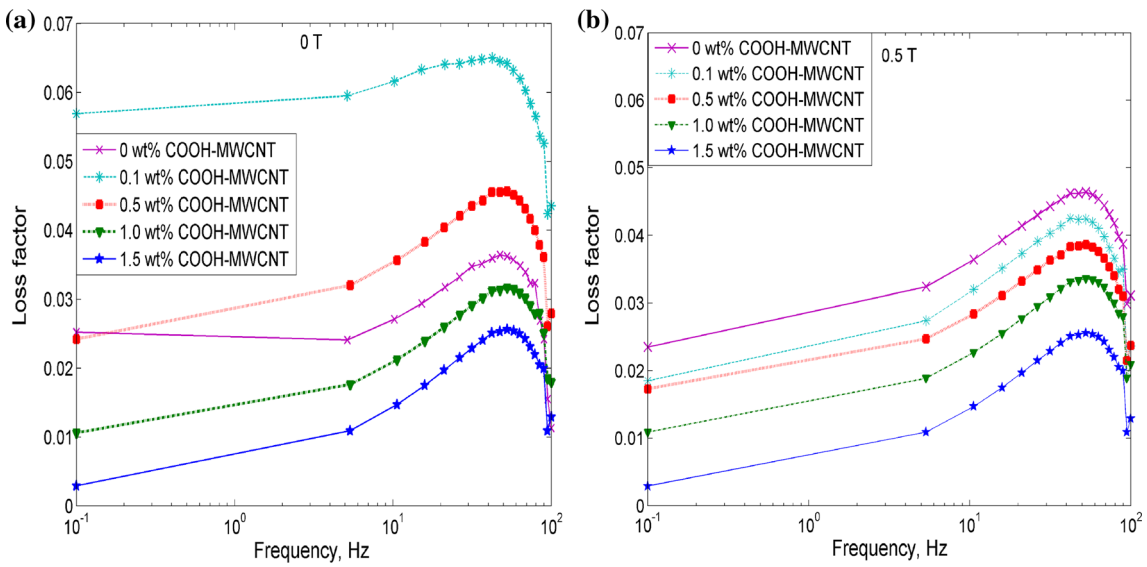

Figure 4 Loss factor vs frequency at **a** 0 T and **b** 0.5 T for different ratios of COOH-MWCNT.

relative motion, which therefore improved the interface damping [34]. At higher frequencies of 60 Hz, all the MRE samples exhibited a sharp decrement in loss factors in both off-state and on-state conditions. A possible explanation towards this phenomenon is the molecular deformation and rearrangement changes as the loss factor is strongly dependent on the movement, alignment and deformation of the particles. High frequencies might slowdown the timescales of these CIPs and COOH-MWCNTs relaxation and rearrangements that are free to reorient in an external field. These contribute to less friction at higher frequencies. This trend is quiet similar to the trend reported by Ondreas et al. [47] which found that with a longer the relaxation time, loss factors occur less with increases of frequency at a constant strain amplitude.

Rheological properties of strain swept of MRE

The variation in storage modulus versus strains with respect to COOH-MWCNT loading is represented in Fig. 5. The relationship between the storage modulus and the strain is important in order to study the filler network structure [48]. Therefore, as shown in Fig. 5, at zero-field magnetic fields, the initial storage modulus of all the MRE samples increased paralleling the increments of COOH-MWCNT loading at a zero magnetic field and 0.5T. However, the gradual decrease in storage modulus was observed for all MRE samples with an increase in strain amplitude, which is related to filler networks breaking down [49]. By comparing MRE samples at different compositions, it can be concluded that the dynamic viscoelastic properties have strain dependence. This is called the Payne effect. The Payne effect revealed that the storage modulus value is largely recoverable upon returning to smaller amplitudes. At 0 T, 1.0 wt% of COOH-MWCNT exhibits the highest storage modulus at about 0.53 MPa, meanwhile at 0.5 T, 0.5 wt% showed the highest storage modulus of 0.50 MPa compared to MREs without COOH-MWCNTs which showed a lower storage modulus for both conditions of 0 and 0.5 T. These results agree well with Subramaniam et al. [50], who reported that the well-developed three-dimensional filler network was formed due to well-dispersed additive/fillers and leads to an increment in storage modulus. In addition, this increment in storage modulus can also be attributed to stronger interactions between COOH-MWCNTs particles and matrices, which make the samples more resistant to deformation. However, the initial storage modulus of 1.0 and 1.5 wt% decreased at a higher magnetic field strength of 0.5 T as compared to 0 T, from 0.53 to 0.49 and 0.51 to 0.49 MPa. Due to a higher loading of COOH-MWCNT, the nanotubes not only fill the void between the CIP but at the same time, begin to hinder the chain structures formed by the CIP as larger numbers of nanotubes get stuck between the

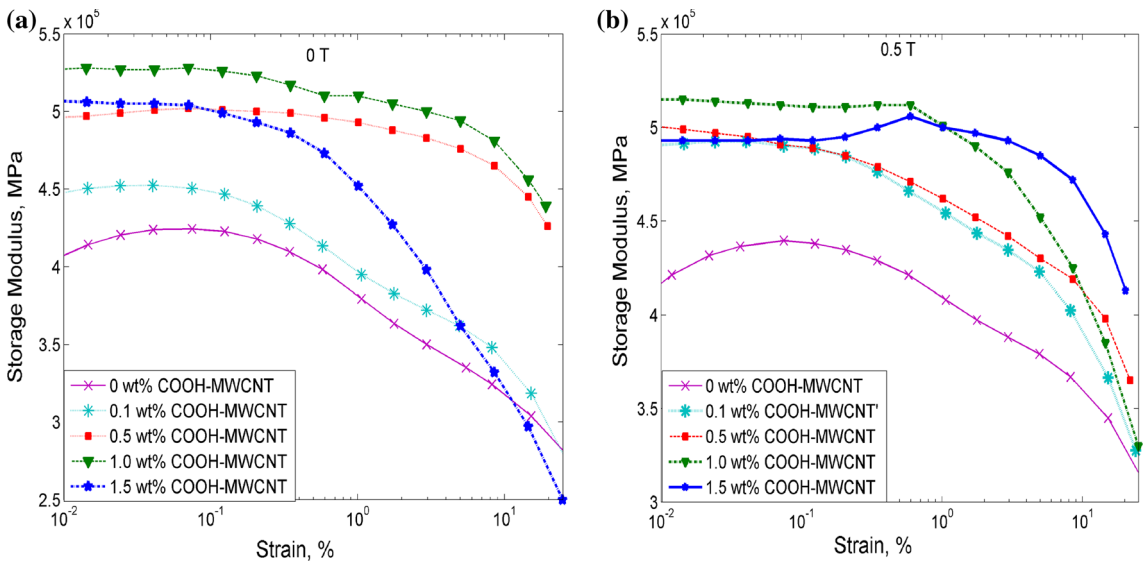

Figure 5 Storage modulus vs strain at **a** 0 T and **b** 0.5 T for different ratios of COOH-MWCNT.

microparticles. This phenomena has been reported and agreed as well by Yu et al. [34].

Loss factor or tan δ, defined as the ratio of loss modulus to storage modulus, is an important parameter in characterizing the macromolecular viscoelasticity and the damping capacity of MRE materials. Figure 6 shows the relationship between loss factor and strain for all MRE samples at both 0 and 0.5 T. All the MRE samples exhibit a smaller loss factor, which refers to small energy dissipation in the MRE samples. The loading of COOH-MWCNT in a MRE influences its damping property. The loss factor graph shows a decreasing graph with increase in COOH-MWCNT loading, indicating that there is a reduction in heat build-up and damping capability of MREs with COOH-MWCNTs loading [41]. MREs with 0.1, 0.5 and 1.5 wt% of COOH-MWCNTs show the highest loss factors at higher strains (> 10%) as compared to MREs without COOH-MWCNTs. Nevertheless, the loss factor of MRE samples containing 1.0 wt% COOH-MWCNTs, exhibit lower loss factors compared to other MRE samples. Obviously, the addition of CNTs up to 1.5 wt% gives a higher loss factor at higher strain. Above this level, the loss factor is reduced. The loading of COOH-MWCNTs in MREs influences the loss factor, which is related to the damping capability. This result is parallel to the previous study done by Liu et al. [42] in which the higher content of COOH-MWCNTs loading increased the maximum damping properties. This is attributed to the stick–slip mechanism, and the frictional sliding of CIP and COOH-MWCNT together with COOH-MWCNT and matrix interactions.

Rheological properties for sweep current

Figure 7 depicts the relationship between the magneto-induced storage modulus and different loadings of COOH-MWCNTs at various magnetic field strength. All MRE samples exhibit increment parallel with the increment of magnetic field strength. The magneto-induced storage modulus is enhanced from 0.38 to 0.46, 0.39 to 0.45, 0.42 to 0.48, 0.46 to 0.54 and 0.43 to 0.46 MPa for MRE without COOH-MWCNT, 0.1, 0.5,1.0 and 1.5 wt% COOH-MWCNT loading, respectively. These results appear to be that the storage modulus is dependent on the COOH-MWCNT loading. When a certain magnetic field strength is imposed, the CIP and COOH-MWCNTs in the MRE samples exhibit magnetic-induced force between particles which provide a resistance deformation, resulting in a change of shear modulus.

As the total number of particles or voids in rubber or MREs matrix is enormous, even small modifications of their local environment will add up to influencing macroscopic (mechanical) performance. These effects and the resulting micromechanical deformations during the deformation of filled multiphase polymers voids or pores were initiated either by cavities inside the rubber particles or by debonding at the matrix–particle interface. The numerous voids tend to favour the plastic deformation

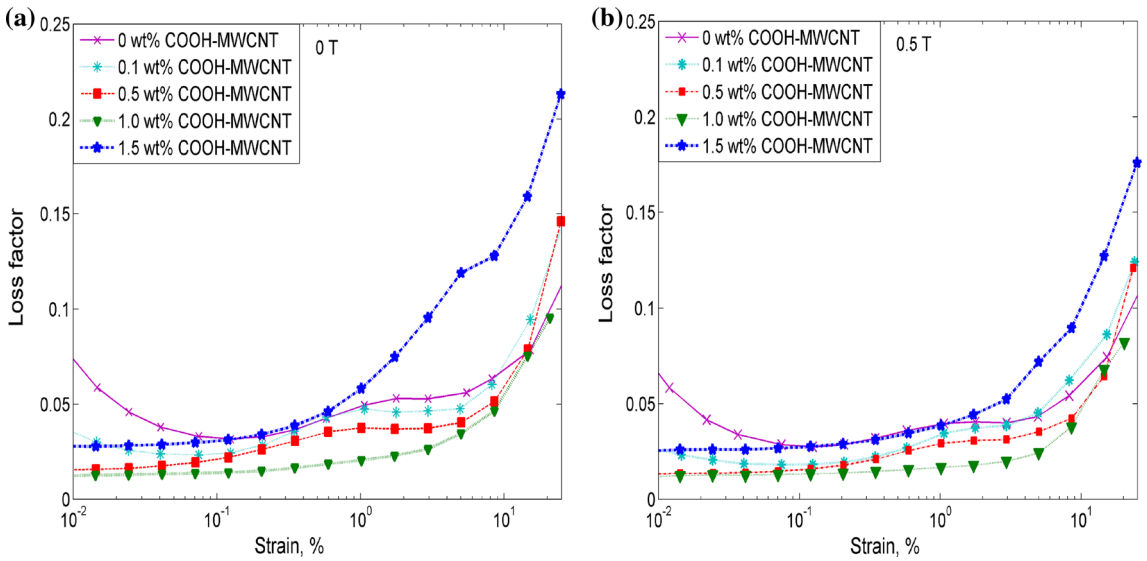

Figure 6 Loss factor vs strain at **a** 0 T and **b** 0.5 T for different ratios of COOH-MWCNT.

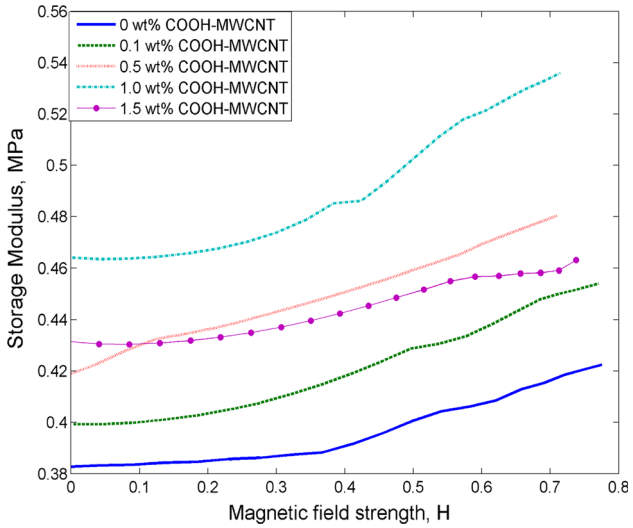

Figure 7 The magneto-induced storage modulus of the MRE samples at different contents of COOH-MWCNT and magnetic flux densities.

phenomena, e.g. crazing or shear band formation in a polymeric matrix at and between rubber particles. This kind of similar phenomenon has been reported previously by Michler et al. [51]. In this case, as the size of COOH-MWCNT is between 10 and 20 nm and lower in content, it reacts as a real toughening agent [51]. In this case, as the COOH-MWCNTs size is between 20 nm, and lower in content, it reacts as a real toughening agent [51], as the COOH-MWCNTs is homogeneously dispersed as shown in Fig. 2. The COOH-MWCNT occupied the void of CIP in MRE thus strengthening the chain-like structures in MRE as shown in Fig. 8. However, at a higher content of 1.5 wt% COOH-MWCNT, it began to hinder the chain structure formed by the spherical particles as higher loading of COOH-MWCNT created higher van der Waals force between fillers which reduces the particle mobility as shown in Fig. 9b.

Therefore, the CIP in matrix shifted hard to form the chain-like structures in the direction of the applied magnetic field. This resulting in a low distribution of COOH-MWCNTs in MRE matrix thus created a reduction in storage and magneto-induced modulus. It is also believed that this interference of the CIP-COOH-MWCNT in the chain-like structures is the reason of the decrement in MR effect at 1.5 wt% COOH-MWCNT content.

The modulus changes in viscoelastic properties of MRE when subjected to a magnetic field are defined as MR effect. The MR effect is related to the magnetic particles tendency to change their position under the influence of applied magnetic field. The movement of particles resulted in an increment of stiffness and shear modulus in MREs. Additionally, the interactions between particles in magnetic field also introduce a deformation in matrix due to their attractions to each other and consequently increase the stiffness of the material and shear modulus. The MR effect can be described by both absolute and relative MR effects. The absolute MR effect (ΔG) is calculated using the difference between the initial modulus G'_0 (zero-field modulus) and the maximum shear modulus, G'_{max} achieved with the applied of a magnetic induction during the test. The absolute MR effect can be described by:

$$\Delta G = G'_{max} - G'_0 \tag{1.1}$$

The relative MR effect is defined as the ratio of absolute MR effect to the initial modulus. The equation is as follows:

$$MR_{effect} = \frac{G'_{max} - G'_0}{G'_0} \times 100\% \tag{1.2}$$

The effect of the absolute and relative MR effect of various loading of COOH-MWCNT was investigated as shown in Table 2.

The MR effect of MRE samples increased with the increasing of COOH-MWCNT content up to 1.0 wt%. Clearly, there is reinforcement as evidenced by considerable improvements in stiffness and absolute MR

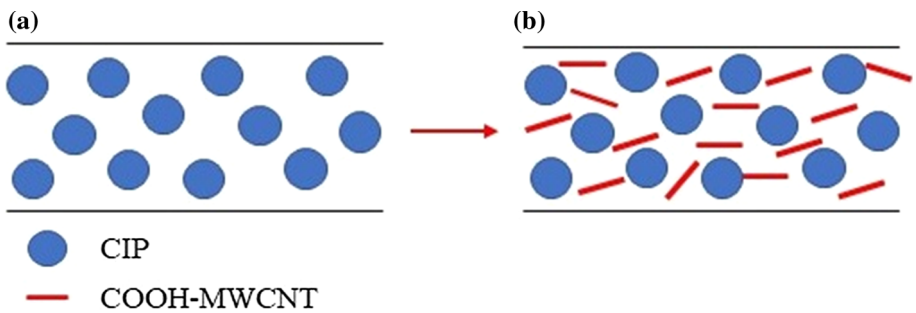

Figure 8 Schematic diagram of partial substitution by COOH-MWCNTs in MRE samples.

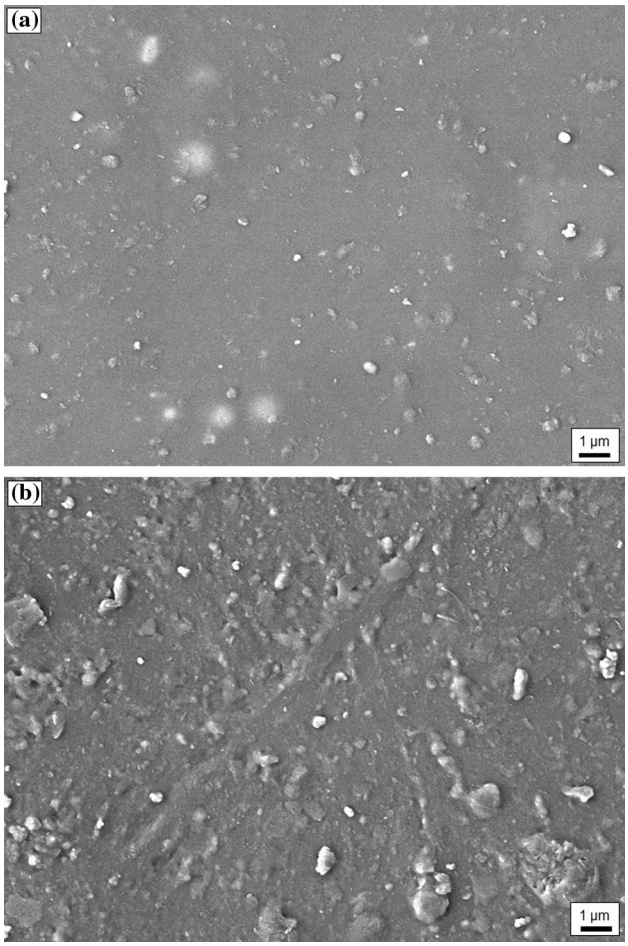

Figure 9 Dispersion of CIPs and COOH-MWCNTs at higher filler loading of **a** 1.0 wt%.

effect with the COOH-MWCNT loading. From all the MRE samples, the 1.0 wt% of COOH-MWCNT exhibits higher MR effect of 17.5% as compared to other MRE samples. This is due to by mixing two different shapes of materials, which will create a synergistic effect in which the COOH-MWCNT was in contact with the CIP and will fill the void of CIP. Therefore, it is assumed that during the current sweep of shear mode test, the COOH-MWCNTs would vibrate and migrate towards the CIPs and matrix phase and form new reinforcement mechanism to increase the magneto-induced modulus of the MRE samples as shown in Fig. 10.

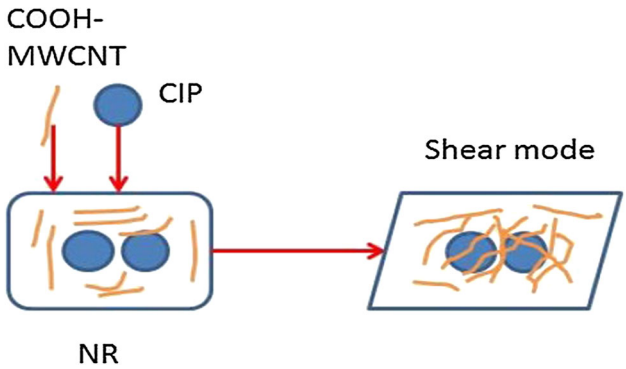

Figure 10 The reinforcement mechanism interaction in MRE.

The reinforcement mechanism of COOH-MWCNT in MRE is related also to the rubber bound that occurs dependence on the loading of COOH-MWCNTs. The almost same phenomena also have been reported by few researchers such as Yang et al., Mordina et al. and Hong et al. [52–54]. In addition, at higher loading COOH-MWCNTs, more interaction will occur between filler and filler compared to filler and matrix which also has been reported by another researcher in the previous study of composites material [55]. However, at 1.5 wt% COOH-MWCNT, the MR effect decreased sharply which might be due to the presence of aggregates increasing at higher filler loading as shown in Fig. 9(b). Further experimental and theoretical studies related to the reinforcement mechanism will need to perform to confirm this trend and hypothesis.

Conclusions

In this work, experimental investigation on various loadings of 0–1.5 wt% of COOH-MWCNT in isotropic MREs has been carried out. The functionalization of MWCNTs has more potentials to be utilized in MRE due to the improvement and uniform

Table 2 Absolute and MR effect of MRE samples at various loading of COOH-MWCNT

Samples	Initial modulus, G' (MPa)	Absolute MR effect, $\Delta G'$	MR effect (%)
Without COOH-MWCNT	0.3827	0.0398	10.4
0.1 wt% COOH-MWCNT	0.3993	0.0547	13.7
0.5 wt% COOH-MWCNT	0.4190	0.0615	14.3
1.0 wt% COOH-MWCNT	0.4614	0.0809	17.5
1.5 wt% COOH-MWCNT	0.4304	0.0327	7.6

dispersion between matrix-CIP and functionalized COOH-MWCNT. Furthermore, a strong interfacial bonding between COOH-MWCNTs and matrix as well as a strong interaction between COOH-MWNTs and CIPs have been observed through micrograph analysis. The added COOH-MWCNTs are capable to enhance the viscoelastic properties of MRE. In addition, the viscoelastic properties of MRE with COOH-MWCNTs have showed a greater initial zero-field storage. Whilst, in another condition, the properties have revealed a bigger storage modulus at a higher loading when the magnetic fields strength is increased. Even though, the applied magnetic field is rapidly increased, the loss factor of MRE with COOH-MWCNTs is slowly decreased. As in comparison with the traditional MREs, the additional of COOH-MWCNTs help to improve the initial modulus, magneto-induced modulus and damping property of MREs. However, these improvements can be achieved at optimum value of 1.0wt % of COOH-MWCNTs, before the viscoelastic properties of MREs began to decrease at a higher value. These findings indicate that MR performance of the fabricated MREs is strongly dependent on the loading amount of the COOH-MWCNTs. In the future works, the reinforcing mechanism and the percolation threshold of MRE with COOH-MWCNT will be further investigated. The study will involve the improvement that related to their mechanical and rheological properties and compare with the influence of nanoscale carbon black.

Acknowledgements

The author gratefully acknowledges the financial funded by the Ministry of Higher Education, Malaysia PRGS (Vot No: 4L667), Universiti Teknologi Malaysia under GUP Grant (Vot No: 13H55), PDRU Grant (Vot No: 04E02) and also Malaysian Rubber Board for their technical advice and facilities, SHERA Project Prime Award: AID-497-A-16-00004, USAID, as well as Universitas Sebelas Maret (UNS) through Hibah Mandatory 2018.

Compliance with ethical standards

Conflict interest The authors declare that there is no conflict of interest.

References

[1] Mazlan SA (2008) The behaviour of magnetorheological fluids in squeeze mode. Dublin City University, Dublin

[2] Yunus NA, Mazlan SA, Ubaidillah et al (2016) Rheological properties of isotropic magnetorheological elastomers featuring an epoxidized natural rubber. Smart Mater Struct 25:107001. https://doi.org/10.1088/0964-1726/25/10/107001

[3] Mohamad N, Mazlan SA, Ubaidillah (2016) Effect of carbonyl iron particles composition on the physical characteristics of MR grease. p 40027

[4] Ubaidillah, Imaduddin F, Li YC et al (2016) A new class of magnetorheological elastomers based on waste tire rubber and the characterization of their properties. Smart Mater Struct 25:1–15. https://doi.org/10.1088/0964-1726/25/11/115002

[5] Zhang W, Gong XL, Xuan SH, Xu YG (2010) High-performance hybrid magnetorheological materials: preparation and mechanical properties. Ind Eng Chem Res 49:12471–12476. https://doi.org/10.1021/ie101904f

[6] Li W, Zhang X (2008) Research and applications of MR elastomers. Recent Patents Mech Eng 1:161–166. https://doi.org/10.2174/2212797610801030161

[7] Carlson JD, Jolly MR (2000) MR fluid, foam and elastomer devices. Mechatronics 10:555–569. https://doi.org/10.1016/S0957-4158(99)00064-1

[8] Jolly MR, Carlson JD, Muñoz BC (1996) A model of the behaviour of magnetorheological materials. Smart Mater Struct 5:607–614. https://doi.org/10.1088/0964-1726/5/5/009

[9] Yu M, Fu J, Ju BX et al (2013) Influence of x-ray radiation on the properties of magnetorheological elastomers. Smart Mater Struct 22:125010. https://doi.org/10.1088/0964-1726/22/12/125010

[10] Kavlicoglu BM, Gordaninejad F, Wang X (2013) Study of a magnetorheological grease clutch. Smart Mater Struct 22:125030. https://doi.org/10.1088/0964-1726/22/12/125030

[11] Boczkowska A, Awietjan SF (2009) Urethane magnetorheological elastomers—manufacturing, microstructure and properties. Solid State Phenom 154:107–112. https://doi.org/10.4028/www.scientific.net/SSP.154.107

[12] Chertovich A, Stepanov G, Kramarenko E, Khokhlov A (2010) New composite elastomers with giant magnetic response. Macromol Mater Eng 295:336–341. https://doi.org/10.1002/mame.200900301

[13] Jiang W, Yao J, Gong X, Chen L (2008) Enhancement in magnetorheological effect of magnetorheological elastomers

by surface modification of iron particles. Chin J Chem Phys 21:87–92. https://doi.org/10.1088/1674-0068/21/01/87-92

[14] Agirre-Olabide I, Elejabarrieta MJ, Bou-Ali MM (2015) Matrix dependence of the linear viscoelastic region in magnetorheological elastomers. J Intell Mater Syst Struct 26:1880–1886. https://doi.org/10.1177/1045389X15580658

[15] Zhu J, Xu Z, Guo Y (2013) Experimental and modeling study on magnetorheological elastomers with different matrices. J Mater Civ Eng 25:1762–1771. https://doi.org/10.1061/(ASCE)MT.1943-5533.0000727

[16] Khimi SR, Pickering KL (2015) Comparison of dynamic properties of magnetorheological elastomers with existing antivibration rubbers. Compos Part B Eng 83:175–183. https://doi.org/10.1016/j.compositesb.2015.08.033

[17] Pickering KL, Raa Khimi S, Ilanko S (2015) The effect of silane coupling agent on iron sand for use in magnetorheological elastomers part 1: surface chemical modification and characterization. Compos Part A Appl Sci Manuf 68:377–386. https://doi.org/10.1016/j.compositesa.2014.10.005

[18] Sui G, Zhong WH, Yang XP et al (2008) Preparation and properties of natural rubber composites reinforced with pretreated carbon nanotubes. Polym Adv Technol. https://doi.org/10.1002/pat.1163

[19] Damiani R (2014) Interface control and viscoelastic behavior of magnetorheological nanocomposites. University of California, Berkeley

[20] Ge L, Gong X, Fan Y, Xuan S (2013) Preparation and mechanical properties of the magnetorheological elastomer based on natural rubber/rosin glycerin hybrid matrix. Smart Mater Struct 22:115029. https://doi.org/10.1088/0964-1726/22/11/115029

[21] Chen L, Gong X, Jiang W et al (2007) Investigation on magnetorheological elastomers based on natural rubber. J Mater Sci 42:5483–5489. https://doi.org/10.1007/s10853-006-0975-x

[22] Ahmad Khairi MH, Mazlan SA, Ubaidillah et al (2017) The field-dependent complex modulus of magnetorheological elastomers consisting of sucrose acetate isobutyrate ester. J Intell Mater Syst Struct 28:1993–2004. https://doi.org/10.1177/1045389X16682844

[23] Wang Y, Zhang X, Oh J, Chung K (2015) Fabrication and properties of magnetorheological elastomers based on CR/ENR self-crosslinking blends. Smart Mater Struct 24:95006. https://doi.org/10.1088/0964-1726/24/9/095006

[24] Sorokin VV, Ecker E, Stepanov GV et al (2014) Experimental study of the magnetic field enhanced Payne effect in magnetorheological elastomers. Soft Matter 10:8765–8776. https://doi.org/10.1039/C4SM01738B

[25] Wu J, Gong X, Fan Y, Xia H (2010) Anisotropic polyurethane magnetorheological elastomer prepared through in situ polycondensation under a magnetic field. Smart Mater Struct 19:105007. https://doi.org/10.1088/0964-1726/19/10/105007

[26] Zhou Y, Jerrams S, Betts A, et al (2013) The effect of microstructure on the dynamic equi- biaxial fatigue behaviour of magnetorheological elastomers. In: 8th European conference on constitutive models for rubbers (ECCMR VIII). pp 25–28

[27] Koo J-H, Dawson A, Jung H-J (2012) Characterization of actuation properties of magnetorheological elastomers with embedded hard magnetic particles. J Intell Mater Syst Struct 23:1049–1054. https://doi.org/10.1177/1045389X12439635

[28] Li GH, Huang XG, Gu XY, Wang J (2013) Fabrication and mechanical properties study of the magnetorheological elastomer. Appl Mech Mater 376:148–152. https://doi.org/10.4028/www.scientific.net/AMM.376.148

[29] Ubaidillah, Sutrisno J, Purwanto A, Mazlan SA (2015) Recent progress on magnetorheological solids: materials, fabrication, testing, and applications. Adv Eng Mater 17:563–597. https://doi.org/10.1002/adem.201400258

[30] Li Y, Li J, Li W, Du H (2014) A state-of-the-art review on magnetorheological elastomer devices. Smart Mater Struct 23:123001. https://doi.org/10.1088/0964-1726/23/12/123001

[31] Aloui S, Klüppel M (2015) Magneto-rheological response of elastomer composites with hybrid-magnetic fillers. Smart Mater Struct 24:25016. https://doi.org/10.1088/0964-1726/24/2/025016

[32] Li Y, Li J, Li W, Samali B (2013) Development and characterization of a magnetorheological elastomer based adaptive seismic isolator. Smart Mater Struct 22:35005. https://doi.org/10.1088/0964-1726/22/3/035005

[33] Chen L, Gong XL, Li WH (2008) Effect of carbon black on the mechanical performances of magnetorheological elastomers. Polym Test 27:340–345. https://doi.org/10.1016/j.polymertesting.2007.12.003

[34] Yu M, Zhu M, Fu J et al (2015) A dimorphic magnetorheological elastomer incorporated with Fe nano-flakes modified carbonyl iron particles: preparation and characterization. Smart Mater Struct 24:115021. https://doi.org/10.1088/0964-1726/24/11/115021

[35] Padalka O, Song HJ, Wereley NM et al (2010) Stiffness and damping in Fe Co, and Ni nanowire-based magnetorheological elastomeric composites. IEEE Trans Magn 46:2275–2277. https://doi.org/10.1109/TMAG.2010.2044759

[36] Li R, Sun LZ (2014) Dynamic viscoelastic behavior of multiwalled carbon nanotube-reinforced magnetorheological

(MR) nanocomposites. J Nanomech Micromech 4:A4013014. https://doi.org/10.1061/(ASCE)NM.2153-5477.0000065

[37] Li R, Sun LZ (2011) Dynamic mechanical behavior of magnetorheological nanocomposites filled with carbon nanotubes. Appl Phys Lett 99:131912. https://doi.org/10.1063/1.3645627

[38] Bica I, Anitas EM, Bunoiu M et al (2014) Hybrid magnetorheological elastomer: influence of magnetic field and compression pressure on its electrical conductivity. J Ind Eng Chem 20:3994–3999. https://doi.org/10.1016/j.jiec.2013.12.102

[39] Landa RA, Soledad Antonel P, Ruiz MM et al (2013) Magnetic and elastic anisotropy in magnetorheological elastomers using nickel-based nanoparticles and nanochains. J Appl Phys 114:213912. https://doi.org/10.1063/1.4839735

[40] Aziz SAA, Mazlan SA, Ismail NIN et al (2016) Effects of multiwall carbon nanotubes on viscoelastic properties of magnetorheological elastomers. Smart Mater Struct 25:77001. https://doi.org/10.1088/0964-1726/25/7/077001

[41] Abdullateef AA, Thomas SP, Al-Harthi MA et al (2012) Natural rubber nanocomposites with functionalized carbon nanotubes: mechanical, dynamic mechanical, and morphology studies. J Appl Polym Sci 125:E76–E84. https://doi.org/10.1002/app.35021

[42] Petriccione A, Zarrelli M, Antonucci V, Giordano M (2014) Aggregates of chemically functionalized multiwalled carbon nanotubes as viscosity reducers. Materials (Basel) 7:3251–3261. https://doi.org/10.3390/ma7043251

[43] Qiu L, Chen Y, Yang Y et al (2013) A study of surface modifications of carbon nanotubes on the properties of polyamide 66/multiwalled carbon nanotube composites. J Nanomater 2013:1–8. https://doi.org/10.1155/2013/252417

[44] Kong I, Ahmad SH, Shanks R (2016) Properties enhancement in multiwalled carbon nanotube-magnetite hybrid-filled polypropylene natural rubber nanocomposites through functionalization and processing methods. Sci Eng Compos Mater 23:257–267. https://doi.org/10.1515/secm-2014-0124

[45] Silva VA, de Folgueras LC, Cândido GM et al (2013) Nanostructured composites based on carbon nanotubes and epoxy resin for use as radar absorbing materials. Mater Res 16:1299–1308. https://doi.org/10.1590/S1516-14392013005000146

[46] Abdul Aziz SA, Mazlan SA, Nik Ismail NI et al (2017) An enhancement of mechanical and rheological properties of magnetorheological elastomer with multiwall carbon nanotubes. J Intell Mater Syst Struct. https://doi.org/10.1177/1045389X17705211

[47] Ondreas F, Jancar J (2015) Temperature, frequency, and small static stress dependence of the molecular mobility in deformed amorphous polymers near their glass transition. Macromolecules 48:4702–4716. https://doi.org/10.1021/acs.macromol.5b00550

[48] Zhang H, Wei Y, Kang Z et al (2017) Influence of partial substitution for CB with MWNTs on performance of CB-filled NR composites. Micro Nano Lett 12:117–122. https://doi.org/10.1049/mnl.2016.0003

[49] Jung HS, Kwon SH, Choi HJ et al (2016) Magnetic carbonyl iron/natural rubber composite elastomer and its magnetorheology. Compos Struct 136:106–112. https://doi.org/10.1016/j.compstruct.2015.10.008

[50] Subramaniam K, Das A, Steinhauser D et al (2011) Effect of ionic liquid on dielectric, mechanical and dynamic mechanical properties of multi-walled carbon nanotubes/polychloroprene rubber composites. Eur Polym J 47:2234–2243. https://doi.org/10.1016/j.eurpolymj.2011.09.021

[51] Michler GH, von Schmeling H-HK-B (2013) The physics and micro-mechanics of nano-voids and nano-particles in polymer combinations. Polymer (Guildf) 54:3131–3144. https://doi.org/10.1016/j.polymer.2013.03.035

[52] Ahmadi M, Shojaei A (2015) Reinforcing mechanisms of carbon nanotubes and high structure carbon black in natural rubber/styrene-butadiene rubber blend prepared by mechanical mixing—effect of bound rubber. Polym Int 64:1627–1638. https://doi.org/10.1002/pi.4964

[53] Hong CH, Kim MW, Zhang WL et al (2016) Fabrication of smart magnetite/reduced graphene oxide composite nanoparticles and their magnetic stimuli-response. J Colloid Interface Sci 481:194–200. https://doi.org/10.1016/j.jcis.2016.07.060

[54] Mordina B, Tiwari RK, Setua DK, Sharma A (2016) Impact of graphene oxide on the magnetorheological behaviour of $BaFe_{12}$ O_{19} nanoparticles filled polyacrylamide hydrogel. Polymer (Guildf) 97:258–272. https://doi.org/10.1016/j.polymer.2016.05.026

[55] Ismail H, Ramly AF, Othman N (2011) The effect of carbon black/multiwall carbon nanotube hybrid fillers on the properties of natural rubber nanocomposites. Polym Plast Technol Eng 50:660–666. https://doi.org/10.1080/03602559.2010.551380